Nuclear Instruments and Methods in Physics Research A 845 (2017) 173–176

Contents lists available at ScienceDirect

Nuclear Instruments and Methods in Physics Research A

journal homepage: www.elsevier.com/locate/nima

Radiation length imaging with high-resolution telescopes

U. Stolzenberg [a,*], A. Frey [a], B. Schwenker [a], P. Wieduwilt [a], C. Marinas [b], F. Lütticke [b]

[a] II. Physikalisches Institut, Universität Göttingen, Friedrich-Hund-Platz 1, 37077 Göttingen, Germany
[b] Physikalisches Institut, Universität Bonn, Nußallee 12, 53115 Bonn, Germany

ARTICLE INFO

Article history:
Received 15 March 2016
Received in revised form
12 June 2016
Accepted 15 June 2016
Available online 16 June 2016

Keywords:
Low mass vertex detector
Multiple scattering
Low mass materials

ABSTRACT

The construction of low mass vertex detectors with a high level of system integration is of great interest for next generation collider experiments. Radiation length images with a sufficient spatial resolution can be used to measure and disentangle complex radiation length X/X_0 profiles and contribute to the understanding of vertex detector systems. Test beam experiments with multi GeV particle beams and high-resolution tracking telescopes provide an opportunity to obtain precise 2D images of the radiation length of thin planar objects. At the heart of the X/X_0 imaging is a spatially resolved measurement of the scattering angles of particles traversing the object under study. The main challenges are the alignment of the reference telescope and the calibration of its angular resolution. In order to demonstrate the capabilities of X/X_0 imaging, a test beam experiment has been conducted. The devices under test were two mechanical prototype modules of the Belle II vertex detector. A data sample of 100 million tracks at 4 GeV has been collected, which is sufficient to resolve complex material profiles on the 30 μm scale.

1. Introduction

Physics requirements limit the mass of vertex and tracking detectors for next generation collider experiments [1]. To meet the conflicting goals of minimising detector mass and also incorporating cooling, power distribution and readout electronics an integrated system design approach is needed [2]. The precision of the measured vertex and track parameters is degraded by multiple scattering effects. The magnitude of multiple scattering depends on the local material budget measured in units of the material constant X_0. It is therefore crucial to carefully limit and account for every material contribution in the detector acceptance region.

In order to study the material composition of planar objects a method has been developed to measure high-resolution 2D images of the radiation length X/X_0. The radiation length can be extracted from the multiple scattering deflections by using an appropriate theoretical model. The good spatial resolution of the method opens a way to measure the overall scattering effect in small areas. It can consequently be used to map fully passive materials very precisely. This provides an opportunity to disentangle material distributions from various different components like ASICs, bump bonds and support structures.

2. Method

For the radiation length measurements the planar object is centred in a high-resolution tracking telescope. A detailed description of the data processing including clustering, alignment and tracking can be found in [3]. The basic idea is to reconstruct multiple scattering angles from charged particle tracks. A pair of Kalman filters can be used to compute the track state and covariance matrix before the scattering η^{in}, C^{in} from the upstream hits and the state and covariance matrix after the scattering η^{out}, C^{out} from the downstream hits. The track states are extrapolated to the scattering plane of the object (u,v,w) and defined as

$$\eta^{\text{in}} = \left((\mathrm{d}u/\mathrm{d}w)^{\text{in}}, (\mathrm{d}v/\mathrm{d}w)^{\text{in}}, u^{\text{in}}, v^{\text{in}} \right)$$
$$\eta^{\text{out}} = \left((\mathrm{d}u/\mathrm{d}w)^{\text{out}}, (\mathrm{d}v/\mathrm{d}w)^{\text{out}}, u^{\text{out}}, v^{\text{out}} \right). \quad (1)$$

While the measurement results are obtained from the optimal weighted mean, for clarity of this text the following formula for the calculation of the intersection point is used, which neglects small correlation effects:

$$u = \left(u^{\text{in}} + u^{\text{out}}\right)/2$$
$$v = \left(v^{\text{in}} + v^{\text{out}}\right)/2 \quad (2)$$

The two projected scattering angles ϑ_i $(i = u, v)$ can be calculated from the difference of track slopes

* Corresponding author.
E-mail address: ulf.stolzenberg@phys.uni-goettingen.de (U. Stolzenberg).

http://dx.doi.org/10.1016/j.nima.2016.06.086
0168-9002/

$$\vartheta_u = \left(\mathrm{d}u/\mathrm{d}w\right)^{\mathrm{out}} - \left(\mathrm{d}u/\mathrm{d}w\right)^{\mathrm{in}} \quad \left(\vartheta_v \text{ analogous}\right) \tag{3}$$

In many cases, the correlation between the estimated scattering angles is very small and can be neglected. The angular resolution can then be computed from the following formula:

$$\sigma_{\mathrm{reso}} = \sqrt{C^{\mathrm{in}}_{\frac{\mathrm{d}u}{\mathrm{d}w}\frac{\mathrm{d}u}{\mathrm{d}w}} + C^{\mathrm{out}}_{\frac{\mathrm{d}u}{\mathrm{d}w}\frac{\mathrm{d}u}{\mathrm{d}w}}} \quad (v \text{ component analogous}) \tag{4}$$

This radiation length estimation approach is based on a X/X_0 estimation technique, which was introduced in [4]. No hit from the scattering planar object is used, therefore the material distribution of any thin object can be analysed. Furthermore due to the track extrapolation from the upstream and downstream side no assumption of the material distribution of the planar object is required.

The object plane is divided into small pixel areas and the tracks are sorted into different pixels according to their intersection point (see Eq. (2)). In order to compute the radiation length value of one pixel of the image the measured angle distribution of this pixel is fitted with the function

$$f_{\mathrm{reco}}(\vartheta) = f_{\mathrm{MSC}} \otimes \frac{1}{\left(\lambda\sigma_{\mathrm{reso}}\right)\sqrt{2\pi}} \exp\left(\frac{-\vartheta^2}{2\left(\lambda\sigma_{\mathrm{reso}}\right)^2}\right) \tag{5}$$

The finite telescope angular resolution σ_{reso} introduces a gaussian error, which broadens the multiple scattering angle distribution f_{MSC}. Hence, the fit function is a convolution between the multiple scattering distribution f_{MSC} and the gaussian error function. The correction factor λ is used to tune the angular resolution for a specific experimental setup to $\lambda \cdot \sigma_{\mathrm{reso}}$ (see Section 3). There are different models to describe multiple scattering distributions f_{MSC}. Two of the most prominent ones were introduced by Moliere [5] and Highland [6]. A recent review of multiple scattering models can be found in [7]. Independently of the model, the width of the angle distribution is determined by the particle momentum p, the thickness X of the material and material properties, which can be reduced to X_0. The width of the angular distribution also depends on the mass of the particle, which can be neglected only for light particles or for high momenta.

3. Experimental setup and calibration

For all the following measurements an AIDA telescope with 6 Mimosa26 (M26) sensors [8] was used. The zero suppression cut of the M26 sensors was tuned in such a way that an equal number of two pixel clusters and one pixel clusters for particle signals is achieved. This gives a hit coordinate resolution for M26 clusters of 3 μm with uncertainties σ_{M26} in the order of roughly 10% [3].

Due to the increased amount of multiple scattering for low energy particles, the method works best with a monoenergetic multi GeV particle beam like for example provided in the DESY test beam facilities. In this case a particle beam of 4 GeV electrons was employed. In preparation for the actual experiment toy studies were conducted to determine the resolution of the reference telescope at the target plane position depending on gaps between the telescope sensors. The selected telescope geometry (see Fig. 1) is a compromise between a good spatial resolution of reconstructed tracks, favoring small spacings between the telescope planes, and a good angular resolution, which improves with the gap size. The spatial resolution of 4 μm is sufficient to resolve even small structures like bump bonds. The angular resolution of 134 μrad on the other hand is good enough to measure angles of 70 μrad, which correspond to the Highland multiple scattering angle width σ_{HL} for a scatterer consisting of 75 μm of silicon at a beam energy of 4 GeV.

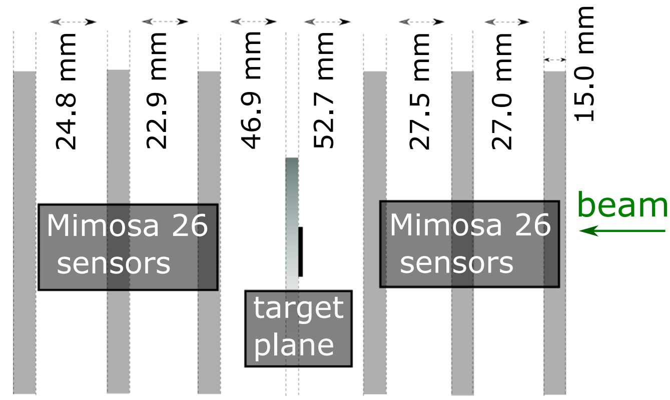

Fig. 1. Experimental setup for X/X_0 imaging. The X/X_0 target is installed between the two arms of a high-resolution reference telescope and is supported perpendicular to the beam axis.

The image pixel size is mainly determined by statistics: Each pixel should have an angle distribution with roughly 1000 entries to ensure a stable fitting with the function in Eq. (5). The exact number of tracks per pixel is also dependent on the fraction between multiple scattering width σ_{HL} and angular resolution σ_{reso}. For materials with a large radiation length fewer tracks per pixel can be used.

For precise X/X_0 measurements it is crucial to know the telescope angular resolution with a very small uncertainty. However, systematical effects like reference telescope alignment, approximations in the tracking model and the uncertainty on the M26 hit reconstruction resolution σ_{M26} are affecting the angular resolution in the measurement plane. The precise determination of the angular resolution with a calibration measurement is therefore vital.

For this purpose a calibrated aluminium target is employed. The calibration target (see lower panel in Fig. 2) is a stack of 9 aluminium layers of 0.2 mm thickness with cutouts. The cutouts define a 3×3 grid of fiducial regions with controlled material thicknesses reaching from air to 1.6 mm aluminium. Three additional fiducial regions have the full thickness of 1.8 mm. While the aluminium target is by far the thickest material in the setup, the energy loss for 4 GeV electrons is still small (<%) and therefore neglected here. The upper panel in Fig. 2 depicts the uncalibrated ($\lambda = 1.0$) X/X_0 image with boxes indicating the 12 regions. During the calibration λ is determined by a simultaneous χ^2 fit of the reconstructed angle distributions in all 12 fiducial regions. For each fit function (Eq. (5)) the thickness is fixed to the reference value. Fig. 3 depicts the reconstructed angle distribution of one of the fiducial regions and the corresponding fit based on the Moliere model (blue curve) and Highland model (red dashed curve). The core and the non-gaussian tail of the reconstructed angle distribution are modelled accurately by the Moliere model. The Highland model can be used to describe the core region of the distribution. For the radiation length measurement the core of the distribution is the most sensitive part. Because of this and the faster fitting procedure the Highland model was used in the following measurements.

For the setup depicted in Fig. 1 the Highland fit yields a λ of 1.152 ± 0.003. The corresponding λ for the Moliere model is 1.165 ± 0.003. The small tension between the two results shows, that for consistent measurements a single multiple scattering model should be used. The composition of systematical effects causing the 15% deviation between expected and real angular resolution is not clear, but small contributions from different sources are expected. Among them are for example telescope misalignment and the uncertainty of the M26 hit position resolution σ_{M26}.